ϕ meson production in $Au + Au$ and $p + p$ collisions at $\sqrt{s_{NN}} = 200$ GeV

J. Adams,[3] C. Adler,[13] M.M. Aggarwal,[27] Z. Ahammed,[40] J. Amonett,[19] B.D. Anderson,[19] D. Arkhipkin,[12] G.S. Averichev,[11] S.K. Badyal,[18] J. Balewski,[15] O. Barannikova,[30,11] L.S. Barnby,[3] J. Baudot,[17] S. Bekele,[26] V.V. Belaga,[11] R. Bellwied,[43] J. Berger,[13] B.I. Bezverkhny,[45] S. Bhardwaj,[31] A.K. Bhati,[27] H. Bichsel,[42] A. Billmeier,[43] L.C. Bland,[2] C.O. Blyth,[3] B.E. Bonner,[32] M. Botje,[25] A. Boucham,[36] A. Brandin,[23] A. Bravar,[2] R.V. Cadman,[1] X.Z. Cai,[35] H. Caines,[45] M. Calderón de la Barca Sánchez,[2] J. Carroll,[20] J. Castillo,[20] D. Cebra,[5] P. Chaloupka,[10] S. Chattopadhyay,[40] H.F. Chen,[34] Y. Chen,[6] S.P. Chernenko,[11] M. Cherney,[9] A. Chikanian,[45] W. Christie,[2] J.P. Coffin,[17] T.M. Cormier,[43] J.G. Cramer,[42] H.J. Crawford,[4] D. Das,[40] S. Das,[40] A.A. Derevschikov,[29] L. Didenko,[2] T. Dietel,[13] W.J. Dong,[6] X. Dong,[34,20] J.E. Draper,[5] F. Du,[45] A.K. Dubey,[16] V.B. Dunin,[11] J.C. Dunlop,[2] M.R. Dutta Majumdar,[40] V. Eckardt,[21] L.G. Efimov,[11] V. Emelianov,[23] J. Engelage,[4] G. Eppley,[32] B. Erazmus,[36] M. Estienne,[36] P. Fachini,[2] V. Faine,[2] J. Faivre,[17] R. Fatemi,[15] K. Filimonov,[20] P. Filip,[10] E. Finch,[45] Y. Fisyak,[2] D. Flierl,[13] K.J. Foley,[2] J. Fu,[44] C.A. Gagliardi,[37] N. Gagunashvili,[11] J. Gans,[45] M.S. Ganti,[40] L. Gaudichet,[36] M. Germain,[17] F. Geurts,[32] V. Ghazikhanian,[6] P. Ghosh,[40] J.E. Gonzalez,[6] O. Grachov,[43] O. Grebenyuk,[25] S. Gronstal,[9] D. Grosnick,[39] M. Guedon,[17] S.M. Guertin,[6] A. Gupta,[18] T.D. Gutierrez,[5] T.J. Hallman,[2] A. Hamed,[43] D. Hardtke,[20] J.W. Harris,[45] M. Heinz,[45] T.W. Henry,[37] S. Heppelmann,[28] B. Hippolyte,[45] A. Hirsch,[30] E. Hjort,[20] G.W. Hoffmann,[38] M. Horsley,[45] H.Z. Huang,[6] S.L. Huang,[34] E. Hughes,[7] T.J. Humanic,[26] G. Igo,[6] A. Ishihara,[38] P. Jacobs,[20] W.W. Jacobs,[15] M. Janik,[41] H. Jiang,[6,20] I. Johnson,[20] P.G. Jones,[3] E.G. Judd,[4] S. Kabana,[45] M. Kaplan,[8] D. Keane,[19] V.Yu. Khodyrev,[29] J. Kiryluk,[6] A. Kisiel,[41] J. Klay,[20] S.R. Klein,[20] A. Klyachko,[15] D.D. Koetke,[39] T. Kollegger,[13] M. Kopytine,[19] L. Kotchenda,[23] A.D. Kovalenko,[11] M. Kramer,[24] P. Kravtsov,[23] V.I. Kravtsov,[29] K. Krueger,[1] C. Kuhn,[17] A.I. Kulikov,[11] A. Kumar,[27] G.J. Kunde,[45] C.L. Kunz,[8] R.Kh. Kutuev,[12] A.A. Kuznetsov,[11] M.A.C. Lamont,[3] J.M. Landgraf,[2] S. Lange,[13] B. Lasiuk,[45] F. Laue,[2] J. Lauret,[2] A. Lebedev,[2] R. Lednický,[11] M.J. LeVine,[2] C. Li,[34] Q. Li,[43] S.J. Lindenbaum,[24] M.A. Lisa,[26] F. Liu,[44] L. Liu,[44] Z. Liu,[44] Q.J. Liu,[42] T. Ljubicic,[2] W.J. Llope,[32] H. Long,[6] R.S. Longacre,[2] M. Lopez-Noriega,[26] W.A. Love,[2] T. Ludlam,[2] D. Lynn,[2] J. Ma,[6] Y.G. Ma,[35] D. Magestro,[26] S. Mahajan,[18] L.K. Mangotra,[18] D.P. Mahapatra,[16] R. Majka,[45] R. Manweiler,[39] S. Margetis,[19] C. Markert,[45] L. Martin,[36] J. Marx,[20] H.S. Matis,[20] Yu.A. Matulenko,[29] C.J. McClain,[1] T.S. McShane,[9] F. Meissner,[20] Yu. Melnick,[29] A. Meschanin,[29] M.L. Miller,[45] Z. Milosevich,[8] N.G. Minaev,[29] C. Mironov,[19] A. Mischke,[25] D. Mishra,[16] J. Mitchell,[32] B. Mohanty,[40] L. Molnar,[30] C.F. Moore,[38] M.J. Mora-Corral,[21] D.A. Morozov,[29] V. Morozov,[20] M.M. de Moura,[33] M.G. Munhoz,[33] B.K. Nandi,[40] S.K. Nayak,[18] T.K. Nayak,[40] J.M. Nelson,[3] P.K. Netrakanti,[40] V.A. Nikitin,[12] L.V. Nogach,[29] B. Norman,[19] S.B. Nurushev,[29] G. Odyniec,[20] A. Ogawa,[2] V. Okorokov,[23] M. Oldenburg,[20] D. Olson,[20] G. Paic,[26] S.K. Pal,[40] Y. Panebratsev,[11] S.Y. Panitkin,[2] A.I. Pavlinov,[43] T. Pawlak,[41] T. Peitzmann,[25] V. Perevoztchikov,[2] C. Perkins,[4] W. Peryt,[41] V.A. Petrov,[12] S.C. Phatak,[16] R. Picha,[5] M. Planinic,[46] J. Pluta,[41] N. Porile,[30] J. Porter,[2] A.M. Poskanzer,[20] M. Potekhin,[2] E. Potrebenikova,[11] B.V.K.S. Potukuchi,[18] D. Prindle,[42] C. Pruneau,[43] J. Putschke,[21] G. Rai,[20] G. Rakness,[15] R. Raniwala,[31] S. Raniwala,[31] O. Ravel,[36] R.L. Ray,[38] S.V. Razin,[11,15] D. Reichhold,[30] J.G. Reid,[42] G. Renault,[36] F. Retiere,[20] A. Ridiger,[23] H.G. Ritter,[20] J.B. Roberts,[32] O.V. Rogachevski,[11] J.L. Romero,[5] A. Rose,[43] C. Roy,[36] L.J. Ruan,[34,2] R. Sahoo,[16] I. Sakrejda,[20] S. Salur,[45] J. Sandweiss,[45] I. Savin,[12] J. Schambach,[38] R.P. Scharenberg,[30] N. Schmitz,[21] L.S. Schroeder,[20] K. Schweda,[20] J. Seger,[9] P. Seyboth,[21] E. Shahaliev,[11] M. Shao,[34] W. Shao,[7] M. Sharma,[27] K.E. Shestermanov,[29] S.S. Shimanskii,[11] R.N. Singaraju,[40] F. Simon,[21] G. Skoro,[11] N. Smirnov,[45] R. Snellings,[25] G. Sood,[27] P. Sorensen,[20] J. Sowinski,[15] H.M. Spinka,[1] B. Srivastava,[30] T.D.S. Stanislaus,[39] R. Stock,[13] A. Stolpovsky,[43] M. Strikhanov,[23] B. Stringfellow,[30] C. Struck,[13] A.A.P. Suaide,[33] E. Sugarbaker,[26] C. Suire,[2] M. Šumbera,[10] B. Surrow,[2] T.J.M. Symons,[20] A. Szanto de Toledo,[33] P. Szarwas,[41] A. Tai,[6] J. Takahashi,[33] A.H. Tang,[2,25] D. Thein,[6] J.H. Thomas,[20] S. Timoshenko,[23] M. Tokarev,[11] M.B. Tonjes,[22] T.A. Trainor,[42] S. Trentalange,[6] R.E. Tribble,[37] O. Tsai,[6] T. Ullrich,[2] D.G. Underwood,[1] G. Van Buren,[2] A.M. VanderMolen,[22] R. Varma,[14] I. Vasilevski,[12] A.N. Vasiliev,[29] S.E. Vigdor,[15] Y.P. Viyogi,[40] S.A. Voloshin,[43] M. Vznuzdaev,[23] W. Waggoner,[9] F. Wang,[30] G. Wang,[7] G. Wang,[19] X.L. Wang,[34] Y. Wang,[38] Z.M. Wang,[34] H. Ward,[38] J.W. Watson,[19] J.C. Webb,[15] R. Wells,[26] G.D. Westfall,[22] C. Whitten Jr.,[6] H. Wieman,[20] R. Willson,[26] S.W. Wissink,[15] R. Witt,[45] J. Wood,[6] J. Wu,[34] N. Xu,[20] Z. Xu,[2] Z.Z. Xu,[34] E. Yamamoto,[20] P. Yepes,[32] V.I. Yurevich,[11] B. Yuting,[25] Y.V. Zanevski,[11] H. Zhang,[45,2] W.M. Zhang,[19] Z.P. Zhang,[34] Z.P. Zhaomin,[34] Z.P. Zizong,[34] P.A. Żołnierczuk,[15] R. Zoulkarneev,[12] J. Zoulkarneeva,[12] and A.N. Zubarev[11]

(STAR Collaboration)

[1] *Argonne National Laboratory, Argonne, Illinois 60439*

[2]Brookhaven National Laboratory, Upton, New York 11973
[3]University of Birmingham, Birmingham, United Kingdom
[4]University of California, Berkeley, California 94720
[5]University of California, Davis, California 95616
[6]University of California, Los Angeles, California 90095
[7]California Institute of Technology, Pasadena, California 91125
[8]Carnegie Mellon University, Pittsburgh, Pennsylvania 15213
[9]Creighton University, Omaha, Nebraska 68178
[10]Nuclear Physics Institute AS CR, Řež/Prague, Czech Republic
[11]Laboratory for High Energy (JINR), Dubna, Russia
[12]Particle Physics Laboratory (JINR), Dubna, Russia
[13]University of Frankfurt, Frankfurt, Germany
[14]Indian Institute of Technology, Mumbai, India
[15]Indiana University, Bloomington, Indiana 47408
[16]Institute of Physics, Bhubaneswar 751005, India
[17]Institut de Recherches Subatomiques, Strasbourg, France
[18]University of Jammu, Jammu 180001, India
[19]Kent State University, Kent, Ohio 44242
[20]Lawrence Berkeley National Laboratory, Berkeley, California 94720
[21]Max-Planck-Institut für Physik, Munich, Germany
[22]Michigan State University, East Lansing, Michigan 48824
[23]Moscow Engineering Physics Institute, Moscow Russia
[24]City College of New York, New York City, New York 10031
[25]NIKHEF, Amsterdam, The Netherlands
[26]Ohio State University, Columbus, Ohio 43210
[27]Panjab University, Chandigarh 160014, India
[28]Pennsylvania State University, University Park, Pennsylvania 16802
[29]Institute of High Energy Physics, Protvino, Russia
[30]Purdue University, West Lafayette, Indiana 47907
[31]University of Rajasthan, Jaipur 302004, India
[32]Rice University, Houston, Texas 77251
[33]Universidade de Sao Paulo, Sao Paulo, Brazil
[34]University of Science & Technology of China, Anhui 230027, China
[35]Shanghai Institute of Nuclear Research, Shanghai 201800, P.R. China
[36]SUBATECH, Nantes, France
[37]Texas A&M University, College Station, Texas 77843
[38]University of Texas, Austin, Texas 78712
[39]Valparaiso University, Valparaiso, Indiana 46383
[40]Variable Energy Cyclotron Centre, Kolkata 700064, India
[41]Warsaw University of Technology, Warsaw, Poland
[42]University of Washington, Seattle, Washington 98195
[43]Wayne State University, Detroit, Michigan 48201
[44]Institute of Particle Physics, CCNU (HZNU), Wuhan, 430079 China
[45]Yale University, New Haven, Connecticut 06520
[46]University of Zagreb, Zagreb, HR-10002, Croatia

We report the STAR measurement of ϕ meson production in $Au + Au$ and $p + p$ collisions at $\sqrt{s_{NN}} = 200$ GeV. Using the event mixing technique, the ϕ spectra and yields are obtained at mid-rapidity for five centrality bins in $Au+Au$ collisions and for non-singly-diffractive $p+p$ collisions. It is found that the ϕ transverse momentum distributions from $Au+Au$ collisions are better fitted with a single-exponential while the $p+p$ spectrum is better described by a double-exponential distribution. The measured nuclear modification factors indicate that ϕ production in central $Au+Au$ collisions is suppressed relative to peripheral collisions when scaled by the number of binary collisions ($\langle N_{bin} \rangle$). The systematics of $\langle p_t \rangle$ versus centrality and the constant ϕ/K^- ratio versus beam species, centrality, and collision energy rule out kaon coalescence as the dominant mechanism for ϕ production.

PACS numbers: 25.75.Dw

In elementary collisions the production of the ϕ meson, the lightest bound state of strange quarks ($s\bar{s}$), is suppressed because of the OZI rule [1, 2, 3]. In heavy-ion collisions, however, strange quarks are produced copiously and ϕ enhancement is observed relative to expectations from $p + p$ collisions [4, 5, 6]. Theoretical calculations have tried to address the origins of this enhancement [7, 8, 9]. The ϕ meson is also thought to have a small hadronic cross-section [10] and may provide direct information about the dense matter at hadron for-

mation without perturbations from co-moving hadrons. For these reasons, ϕ production in relativistic nuclear collisions has been of great interest.

The mechanism for ϕ production in high energy collisions has remained an open issue. A naive interpretation of the ϕ enhancement observed in heavy-ion collisions would be that the ϕ is produced hadronically via $K\bar{K} \rightarrow \phi$. Hadronic rescattering models such as RQMD and UrQMD [11, 12], implementing such processes, predict an increase in the ϕ/K^- ratio as a function of the number of participants. Rescattering models also predict similar increases in the $\langle p_t \rangle$ of the proton and ϕ meson.

The nuclear modification factors (R_{AA} and R_{CP}) of the ϕ meson are important in differentiating between mass and particle species ordering. Current measurements of identified hadrons by STAR (Λ and K^0_S) show that R_{CP} for the Λ differs from that of the K^0_S [13]. It is difficult, however, to determine whether this difference is related to the mass of the particle or the type of the particle (whether it is a baryon or a meson) since there is a significant mass difference between the Λ and the K^0_S. The ϕ, however, has a mass that is similar to that of the Λ, yet is a meson. A direct comparison of the ϕ R_{CP} and R_{AA} with these previous measurements will provide more insight into this mass vs. particle species dependence.

The STAR detector [14] consists of several sub-systems in a large solenoidal analyzing magnet. For the data taken during the second RHIC run (2001-2002) presented here, the experimental setup consisted of a Time Projection Chamber (TPC), a Central Trigger Barrel (CTB), a pair of Beam-Beam Counters (BBC), and two Zero Degree Calorimeters (ZDC). The ZDC's are used as the experimental trigger for $Au+Au$ collisions while the BBC's are used for the $p+p$ trigger.

The results presented here were obtained from about 2.1 million minimum-bias $Au+Au$ events, 1.1 million central $Au+Au$ events and 6.5 million non-singly-diffractive (NSD) $p+p$ events. Reconstruction of the ϕ was accomplished by calculating the invariant mass (m_{inv}), transverse momentum (p_t), and rapidity (y) of pairs that formed from all permutations of candidate K^+ with K^-. The resulting m_{inv} distribution consisted of the ϕ signal atop a large background that is predominantly combinatorial. The shape of the combinatorial background was calculated using the mixed-event technique [15, 16].

For the centrality measurement, the raw hadron multiplicity distribution within a pseudo-rapidity window $|\eta| \leq 0.5$ is divided into five bins corresponding to 50–80%, 30-50%, 10–30%, top 10% and top 5% of the measured cross section for $Au+Au$ collisions. Events are selected with a primary vertex z position from the center of the TPC of $|z| < 25$ cm for $Au+Au$ collisions and $|z| < 50$ cm for $p+p$ collisions, where z is along the beam axis. These events are further divided according to z to reduce acceptance-induced distortions in the mixed-event background. Correlations in the background due to elliptic flow were minimized by mixing events with similar reaction plane angles. Consistent results are obtained when we construct the background distribution using like-sign pairs from the same-event.

Particle identification (PID) is achieved by correlating the ionization energy loss (dE/dx) of charged particles in the TPC gas with their measured momentum. The measured $\langle dE/dx \rangle$ is reasonably well described by the Bethe-Bloch function [10, 17] smeared with a resolution of width σ. Tracks within 2σ of the kaon Bethe-Bloch curve are selected for this analysis.

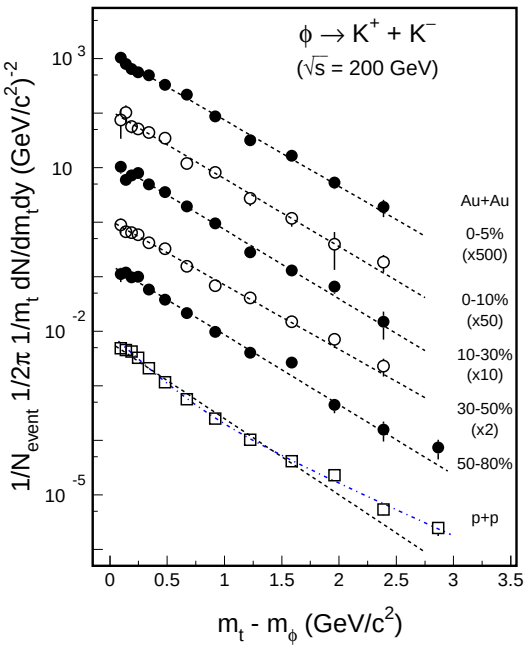

FIG. 1: The transverse mass distributions from $Au+Au$ (circles) and $p+p$ (squares) collisions at 200 GeV. For clarity, some $Au+Au$ distributions for different centralities are scaled by factors. The top 5% data are obtained from the central trigger data set. All other distributions are obtained from the minimum-bias data set. Dashed lines represent the exponential fits to the distributions and the dotted-dashed line is the result of a double-exponential fit to the distribution from $p+p$ collisions. Error bars are statistical errors only.

To obtain the ϕ spectra, same-event and mixed-event distributions are accumulated and background subtraction is done in each p_t, y and centrality bin. The mixed-event background m_{inv} distribution is normalized to the same-event m_{inv} distribution in the region above the ϕ mass ($1.04 < m_{inv} < 1.2$ GeV/c^2). A small, smooth residual background can remain near the ϕ peak in the subtracted m_{inv} distribution, because the mixed-event sample does not perfectly account for the production of background pairs (kaons and/or pions from PID leak-through) that are correlated, either by Coulomb or other interactions or by such instrumental effects as track merging [18]. The raw yield in each bin is then determined by fitting the background subtracted m_{inv} distribution to a Breit-Wigner function plus a linear background in

a limited mass range. The measured mass and width of the ϕ are consistent with the value listed by the Particle Data Group [17] convoluted with detector resolution.

Using GEANT and detector response simulations, the data are corrected for acceptance, kaon decay and tracking efficiencies to obtain the final distributions presented here. Figure 1 shows the transverse mass distributions from $Au+Au$ (circles) and NSD $p+p$ (squares) collisions at 200 GeV. The spectra are obtained from the rapidity range $|y_\phi| < 0.5$. For clarity, some $Au+Au$ distributions for different centralities are scaled by factors indicated in the figure. Dashed lines represent exponential fits to the distributions and the dotted-dashed line represents a double-exponential fit to the $p+p$ result.

Statistical uncertainties are shown in the figure and the results of the fits are listed in Table I. The main contributions to the systematic uncertainty come from fitting to the K^+K^- invariant-mass distribution, tracking and the PID efficiency calculation. Different background functions and normalization factors for the mixed-event background were used to determine the uncertainty in the fitting to the invariant-mass distribution and is estimated to be about 5%. The uncertainty from tracking and PID efficiency is estimated, by varying the tracking and PID cuts on the daughter tracks, to be 8%. The overall systematic uncertainty in the yield, dN/dy and $\langle p_t \rangle$ is estimated to be 11%, and includes an additional contribution from fitting the transverse momentum distributions. For $Au+Au$ collisions, the inverse slope parameters and yields are extracted from a single exponential function fit. For $p+p$ collisions, however, there is an additional component beyond a single exponential, see dashed-line in figure 1. The power-law shape provides a better fit at the higher p_t region but failed at low p_t. Double-exponential function provided a better fit so it was used to extract the values of dN/dy and $\langle p_t \rangle$ for the $p+p$ collisions. For the heavy ion results, a Boltzmann distribution and a thermal+flow model [19] are also used to fit the data as a check of the systematic uncertainty in the extrapolated yield and $\langle p_t \rangle$. The systematic uncertainty is $\sim 15\%$ in the overall normalization and $\leq 5\%$ in mean p_t for the $p+p$ data, including uncertainties in the vertex efficiency for very low multiplicity events.

The system-size and beam-energy dependence of $\langle p_t \rangle$, ϕ/K^- and ϕ/h^- are shown in figure 2. For comparison, the $\langle p_t \rangle$ of the $\bar{p}$, K^- and π^- are also shown [20]. In the ϕ/h^- ratio at $\sqrt{s_{NN}} = 200$ GeV shows no significant dependence on centrality for $Au+Au$ collisions, but decreases by about 30% for $p+p$ collisions, see open symbols in plot (b). As a function of energy, see plots (c) and open circles in plot (d), both values of $\langle p_t \rangle$ and ϕ/h^- ratio increase. This indicates that the production of ϕ mesons is sensitive to the initial conditions of the collision.

The general trend for $\bar{p}$, K^- and π^- is an increase in $\langle p_t \rangle$ as a function of centrality, which is indicative of an increased transverse radial flow velocity component to these particles' momentum distributions. The

Centrality	Slope (MeV)	$\langle p_t \rangle$ (GeV/c)	dN/dy
0–5%	363 ± 8	0.97 ± 0.02	7.70 ± 0.30
0–10%	357 ± 14	0.95 ± 0.03	6.65 ± 0.35
10–30%	353 ± 8	0.97 ± 0.02	3.82 ± 0.19
30–50%	383 ± 10	1.02 ± 0.03	1.72 ± 0.06
50–80%	344 ± 9	0.94 ± 0.02	0.48 ± 0.02
$p+p$ minbias	$--$	0.82 ± 0.03	0.018 ± 0.001

TABLE I: Results of ϕ meson inverse slope parameter, $\langle p_t \rangle$, and dN/dy from NSD $p+p$ and $Au+Au$ collisions at RHIC. An exponential is used for the $Au+Au$ data while a double-exponential fit is used for the $p+p$ data. All values are for $|y| < 0.5$ and only statistical errors are quoted.

ϕ $\langle p_t \rangle$, however, shows no significant centrality dependence. This indicates that the ϕ does not participate in the transverse radial flow as does the $\bar{p}$, K^- and π^-. This is expected if the ϕ decouples early on in the collision before transverse radial flow is completely built up. If the ϕ hadronic scattering cross section is much smaller than that of other particles, one would not expect the ϕ $\langle p_t \rangle$ distribution to be appreciably affected by any final state hadronic rescatterings. In contrast to these observations, the RQMD predictions of $\langle p_t \rangle$ for kaon, proton and ϕ all increase as functions of centrality [11, 21].

The yield ratio ϕ/K^- from this analysis is constant as a function of centrality and species ($p+p$ or $Au+Au$). In fact, for collisions above the threshold for ϕ production, the ϕ/K^- ratio is essentially independent of system size, e^+e^- to nucleus-nucleus, and energy from a few GeV up to 200 GeV (Figure 2 (d)) [4, 5, 6, 17, 22, 23, 24]. This is remarkable, considering that the initial conditions of an e^+e^- collision are so drastically different from $Au+Au$ collisions. This observation may indicate that the ratio is dominated by the hadronization process.

Rescattering models (RQMD [11], UrQMD [12]) predict that about 2/3 of ϕ mesons come from kaon coalescence in the final state. The centrality dependence of the ϕ/K^- ratio alone provides a serious test of the current rescattering models. In these models, such as UrQMD, rescattering channels for ϕ production includes $K\bar{K}$ and K-Hyperon modes and predicts an increasing ϕ/K^- ratio vs. centrality. These models also predict an increase in $\langle p_t \rangle$ for the proton, kaon, and ϕ of 40 to 50% from peripheral to central collisions. A comparison of the data to these models does not support the kaon coalescence production mechanism for ϕ mesons.

The particle-type dependence of the nuclear modification factors R_{AA} and R_{CP} [13, 25] should be sensitive to the production dynamics and the hadronization process [26, 27, 28, 29, 30]. R_{AA} is the ratio of the differential yield in a centrality class of $Au+Au$ collisions to the inelastic differential cross-section in $p+p$ collisions, scaled by the overlap integral $T_{AA} = \langle N_{bin} \rangle / \sigma_{inel}$ from a Glauber calculation[31]. The Glauber calculation was performed with $\sigma_{inel} = 42 \pm 1$ mb. The inelastic differ-

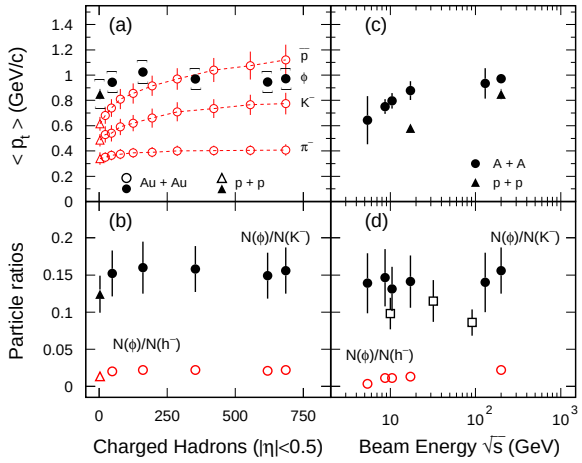

FIG. 2: (a) ϕ $\langle p_t \rangle$ vs. measured number of charged hadrons (N_{ch}) within $|\eta| \leq 0.5$ at 200 GeV. For comparison, the values of $\langle p_t \rangle$ for negative pions, kaons, and anti-protons are also shown; (b) Ratios of N(ϕ)/N(K^-), filled symbols, and N(ϕ)/N(h^-), open symbols, vs. N_{ch}; (c) $\langle p_t \rangle$ vs. center-of-mass beam energy from central nucleus-nucleus (filled circles) and $p+p$ collisions (filled triangles); (d) Ratios of N(ϕ)/N(K^-) from central nucleus-nucleus collisions, filled circles, and N(ϕ)/N(h^-), open circles, vs. center-of-mass beam energy. N(ϕ)/N(K^-) ratio from e^+e^- collisions (open squares) are also shown. Note: All plots are from mid-rapidity. Both the statistical and systematic errors are shown for the 200 GeV STAR data, while only statistical errors are shown for the energy dependence of the particle ratios.

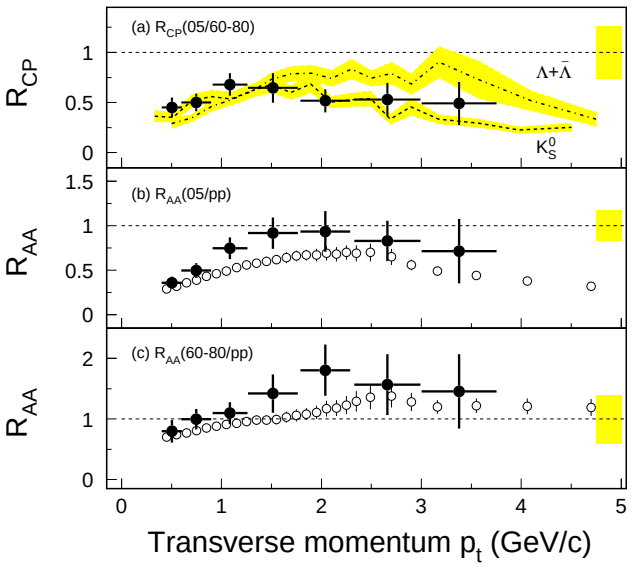

FIG. 3: R_{CP} (a): The ratio of central (top 5%) over peripheral (60-80%) (R_{CP}) normalized by $\langle N_{bin} \rangle$. The ratios for the Λ and K^0_S, shown by dotted-dashed and dashed lines, are taken from [13]; R_{AA} (b) and (c) are the ratios of central $Au+Au$ (top 5%) to $p+p$ and peripheral $Au+Au$ (60-80%) to $p+p$, respectively. The values of R_{AA} for charged hadrons are shown as open circles [25]. The width of the gray bands represent the uncertainties in the estimation of $\langle N_{bin} \rangle$ summed in quadrature with the normalization uncertainties of the spectra. Errors on the ϕ data points are the statistical plus 15% systematic errors.

ential cross-section in $p+p$ is estimated as the NSD yield times σ_{NSD}, measured as 30.0 ± 3.5 mb, with a small correction, determined from Pythia calculations, of 1.05 at pt=0.4 GeV/c and unity above 1.2 GeV/c [25]. R_{CP} is the ratio of the yields between two Au+Au centrality classes, scaled by $\langle N_{bin} \rangle$. The R_{CP} (Figure 3(a)) for the ϕ meson at moderate p_t ($1.5 < p_t < 4$ GeV/c) is suppressed relative to the binary collision scaling (dashed horizontal line at unity).

A comparison of the R_{CP} for the ϕ, K^0_S and Λ is shown in figure 3 (a). Both statistical and systematic errors are included in the figure. The ratio R_{AA} for central (top 5%) and peripheral (60-80%) $Au+Au$ data are shown in Figure 3 (b) and (c), respectively. R_{AA} for charged hadrons [25] is also shown as a reference. The charged hadron and ϕ peripheral R_{AA} both go above the binary scaling limit, but are consistent with unity within the systematic uncertainties. The ϕ central R_{AA} approaches unity and point to point is higher than R_{CP}. With the systematic uncertainty on the normalization of the ratio, however, both R_{AA} and R_{CP} are consistent. Note that a R_{AA} ratio that is higher than the R_{CP} ratio would be consistent with OZI suppression of ϕ production in $p+p$ [1, 2, 3] and/or strangeness enhancement in $Au+Au$ collisions. A measurement of R_{AA} vs. system size may be sensitive to the system size at which OZI becomes irrelevant to ϕ production.

The ϕ R_{CP} result is consistent with a partonic recombination scenario [30, 32, 33]. In these models, the centrality dependence of the yield at intermediate p_t depends more strongly on the number of constituent quarks than on the particle mass. Further higher statistical data for the ϕ are needed to draw a conclusion.

In summary, STAR has measured ϕ meson production in $\sqrt{s_{NN}} = 200$ GeV $Au+Au$ and NSD $p+p$ collisions at RHIC. The ϕ/K^- yield ratios from e^+e^-, $p+p$ and $A+A$ collisions over a broad range of collision energy above the ϕ production threshold are remarkably close to each other. ϕ production, when scaled by the number of binary collisions, is suppressed with respect to peripheral collisions in central $Au+Au$ collisions. The lack of a significant centrality dependence of the ϕ/K^- ratio and the values of ϕ $\langle p_t \rangle$ effectively rule out kaon coalescence as a dominant production channel for the ϕ at this energy.

We thank the RHIC Operations Group and RCF at BNL, and the NERSC Center at LBNL for their support. This work was supported in part by the HENP

Divisions of the Office of Science of the U.S. DOE; the U.S. NSF; the BMBF of Germany; IN2P3, RA, RPL, and EMN of France; EPSRC of the United Kingdom; FAPESP of Brazil; the Russian Ministry of Science and Technology; the Ministry of Education and the NNSFC of China; SFOM of the Czech Republic, FOM and UU of the Netherlands, DAE, DST, and CSIR of the Government of India; the Swiss NSF.

[1] S. Okubo, Phys. Lett. **5**, 165 (1963).
[2] G Zweig, CERN Report No 8419/TH412 (1964).
[3] J. Iizuka *et al.*, Prog. Theor. Phys. **35**, 1061 (1966).
[4] B.B. Back *et al.*, nucl-ex/0304017 (2003).
[5] S.V. Afanasiev *et al.*, Phys. Lett. **B491**, 59 (2000).
[6] C. Adler *et al.*, Phys. Rev. **C65**, 041901(R) (2002).
[7] A.J. Baltz and C. Dover, Phys. Rev. **C53**, 362 (1996).
[8] A. Shor, Phys. Rev. Lett. **54**, 1122 (1985).
[9] H. Sorge *et al.*, Phys. Lett. **B289**, 6 (1992).
[10] D. H. Perkins, "Introduction to High Energy Physics", Cambridge University Press, Fourth Edition (2000).
[11] H. Sorge, Phys. Rev. **C52**, 3291 (1995).
[12] M. Bleicher *et al.*, J. Phys. G: Nucl. Part. Phys. **25**, 1859 (1999) and S.A. Bass *et al.*, Phys. Rev. **C60**, 021902 (1999).
[13] J. Adams *et al.* (STAR Collaboration), Phys. Rev. Lett. **92**, 052302 (2004).
[14] K.H. Ackerman *et al.*, Nucl. Instr. Meth. in Phys. Res. **A499**, 624 (2003).
[15] D. L'Hote, Nucl. Inst. Meth. in Phys. Res. **A337**, 544 (1994).
[16] D. Drijard, H. G. Fischer and T. Nakada, Nucl. Inst. Meth. in Phys. Res. **A225**, 367(1984).
[17] K. Hagiwara *et al.*, Phys. Rev. **D66**, 010001 (2002) and references within.
[18] E. Yamamoto, Ph.D. Thesis, University of California - Los Angeles, (2001) (unpublished).
[19] E. Schnedermann, J. Sollfrank and U. Heinz, Phys. Rev. **C48**, 2462 (1993).
[20] J. Adams *et al.*, Phys. Rev. Lett. , in print, (2004).
[21] Y. Cheng *et al.*, Phys. Rev. **C68**, 034910 (2003).
[22] L. Ahle *et al.*, Phys. Rev. **C58**, 3523 (1998).
[23] S.V. Afanasiev *et al*, Phys. Rev. **C66**, 054902 (2002).
[24] K. Adcox *et al.*, Phys. Rev. Lett. **88**, 192302 (2002).
[25] J. Adams *et al.*, Phys. Rev. Lett. **91**, 172302 (2003).
[26] Z. Lin and C.M. Ko, Phys. Rev. Lett. **89**, 202302 (2002).
[27] S.A. Voloshin, Nucl. Phys **A715**, 379c (2003).
[28] D. Molnar and S.A. Voloshin, Phys. Rev. Lett. **91**, 092301 (2003).
[29] V. Greco, C.M. Ko and P. Levai, Phys. Rev. Lett. **90**, 202302 (2003).
[30] R.J. Fries, B. Müller, C. Nonaka and S.A. Bass, Phys. Rev. Lett. **90**, 202303 (2003); and Phys. Rev. **C68**, 044902 (2003).
[31] J. Adams *et al.* nucl-ex/0311017, submitted to Phys. Rev. C.
[32] K.P. Das and R. C. Hwa, Phys. Lett. **68B**, 459 (1977).
[33] R. C. Hwa and C. B. Yang, Phys. Rev. **C67**, 064902 (2003).